CHARACTERIZING INTERNAL POROSITY OF 3D-PRINTED FIBER REINFORCED MATERIALS

Frye L. Mattingly[1,2], Alan Franc[2,3], Vlastamil Kunc[1,2], Chad Duty[1,2]
[1] University of Tennessee, Knoxville
[2] Manufacturing Demonstration Facility, Oak Ridge National Laboratory
[3]Techmer PM, Clinton Tn.

ABSTRACT

As the functional requirements for 3D printed parts become more demanding, the use of fiber reinforced materials in material extrusion printers is increasingly common. Although fiber-reinforced thermoplastics offer higher stiffness and strength, the internal volume of the extruded material often has a high degree of porosity which can negatively impact mechanical properties. This research surveys the internal porosity present across a range of material extrusion additive manufacturing platforms, primarily those involving a single screw extruder, such as the Big Area Additive Manufacturing (BAAM) system. The porosity within the volume of an extruded bead was quantified through image analysis of cross sectional micrographs. The impact of extrusion rate, transient vs steady state flow, multiple hardware configurations, and material conditions were evaluated. Across the five systems studied porosities ranged from 0.1% to 18.4% with the greatest reductions in porosity coming from two systems that added a vent to the extruder barrel which lowered porosity 64% in one case and 98% in the other.

1. INTRODUCTION

One of the most ubiquitous problems within the field of polymer-based Additive Manufacturing (AM) is that of porosity or internal voids. When looking at a cross-section of a printed part, the beads of material look like bricks in a wall. Most other work on porosity has been focused on the gaps or "mortar" between the beads or "bricks." This study is instead focusing on characterizing the porosity within the beads themselves, effectively studying the quality of the "bricks." These two types of porosity can be seen in Figure 1. The initial motivation for this study was that internal porosity of varying magnitudes had been observed for years within samples studied at Oak Ridge National Laboratory's (ORNL) Manufacturing Demonstration Facility (MDF), but the source and variability of the porosity was not clearly understood. Several questions were posed that this study will address. How widespread is porosity in 3D printed fiber-reinforced polymers? What factors affect the magnitude of the porosity? By controlling those factors, can the porosity be reduced or eliminated?

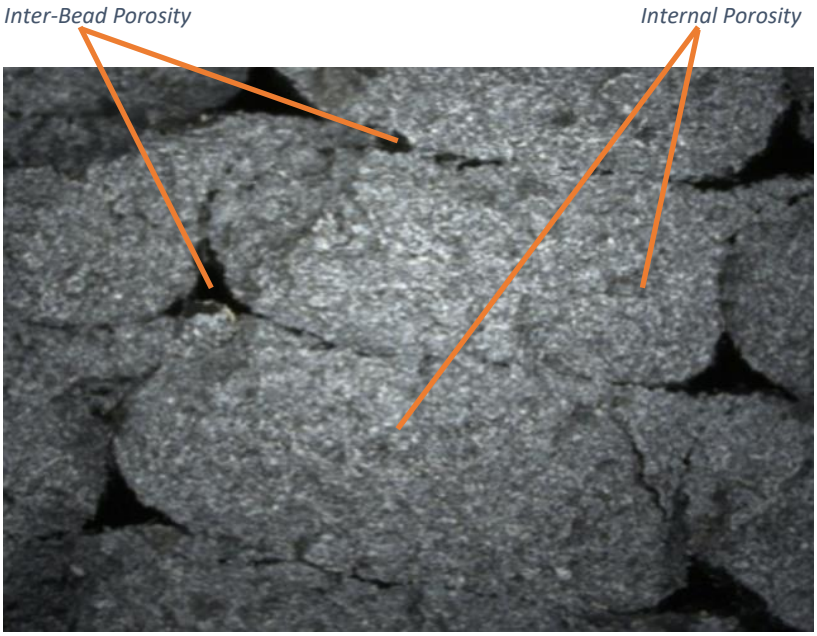

Figure 1, Sample extruded on the BAAM at ORNL's MDF

1.1 Background

The large scale AM systems studied at the MDF are single screw material extruders. Because this technology was developed and modified from equipment used in the Injection Molding (IM) industry, a first step to understanding the issues facing AM is to examine similar issues within IM. A reference book on the subject, "Polymer Extrusion", [1] dedicated several sections to the issue of air entrapment causing voids in molded parts. The text describes four methods of troubleshooting or reducing the voids.

1. Adjust the temperature of the barrel and/or screw.
2. Increase the die pressure to keep the gases in solution.
3. Change the geometry of the screw or barrel to more rapidly pressurize the melting polymer.
4. Design a vent to extract gases prior to the final extrusion.

From these steps we can discern three key factors that carry over to AM: trapped gasses, temperature, and pressure. Unfortunately, in AM polymers are extruded from the printhead directly into atmospheric pressures rather than into a pressurized mold like in IM. This means that even if the internal pressure was dramatically increased, the material would still be molten when exposed to atmospheric pressure allowing trapped gasses to leave solution and expand. Temperature and gas entrapment are readily controllable as can be seen in the field of polymer foams. For example, Nikitine wrote in 2009 [2] how increasing gas solubility and temperature increased porosity. While the purpose of this study is to reduce porosity, not magnify it, papers such as this are a valuable resource into understanding one method through which porosity can form.

Points three and four require redesigns of the extruder screw and barrel but are still worth considering. "Polymer Extrusion" provides an overview of both modified and unmodified single screws. A basic screw consists of three regions along the length of the screw: feed, compression,

and metering (Figure 2). Adding a vent to allow gasses to escape the system requires adding a low pressure region after the initial compression region, but before the final metering section. Figure 3 shows two methods for extracting those gasses from the venting section once the material is depressurized and the gasses have been allowed to leave solution. One option is a simple port on the side of the barrel. This is the simplest solution but requires the modification of the barrel itself as well as a method to seal the vent port if the vent is to be disabled. The second is a hollow screw with a bore hole into the root of the screw channel allowing gasses to escape through the rear of the screw. This method could potentially be retrofitted to a system with minimal changes to the barrel or other components assuming the original barrel was long enough.

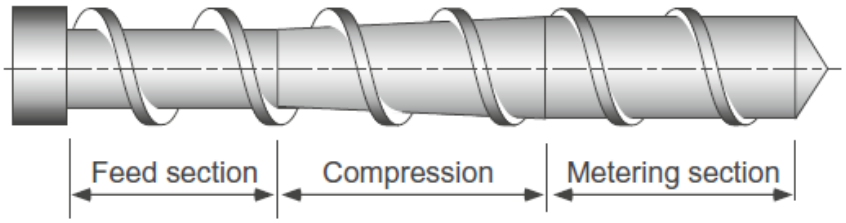

Figure 2, Basics of an Extruder Screw [1]

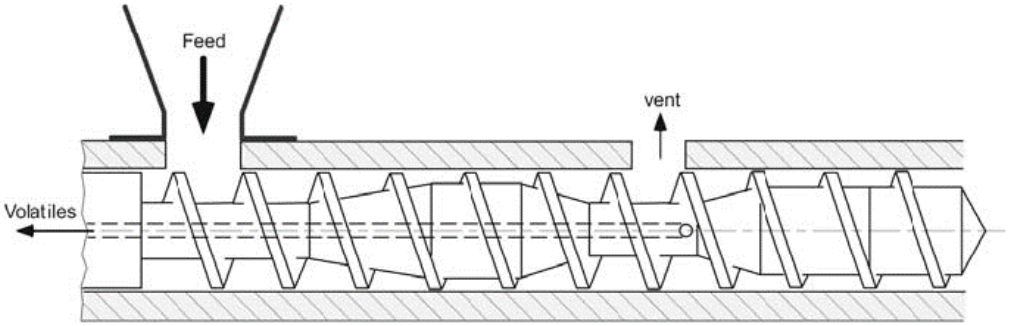

Figure 3, Dual Vented Screw [1]

As a further note on trapped gasses, research at Purdue [3] found that entrapped air is only a partial cause of the porosity seen within AM. After applying a vent porosity was reduced but not entirely eliminated. Non vented samples on this system ranged from 16-27 % porosity and the paper suggested high extrusion rates as another potential source of the porosity for the fiber reinforced polymers being tested. This was attributed to high shear rates damaging fibers and not allowing trapped gases to escape the melt.

1.2 Mechanical Properties

It was generally accepted within literature that porosity would reduce mechanical properties. For example, a 2000 paper on glass fiber thermoplastics in compression molding [4] described a series of tests to show how increasing molding pressure reduced porosity to around 1.9 % and described this as a still significant amount. The previously mentioned paper from Purdue [3] mentions how porosity affects mechanical properties, and attributes the majority of the problem to the porosity between layers rather than to the porosity within the beads themselves.

A few papers that isolate internal porosities from the interlayer porosities were from related fields. One was a study using finite element analysis to study the effects of porosities on crack growth in polymer composites [5]. This paper showed that voids reduced stiffness and that under very specific types of crack growth could improve the tensile properties by increasing the strain-to-failure. A second paper [6] also focusing on FEA analysis showed a near linear relationship between increasing porosity and decreasing relative stiffness in polymer foams.

The third was an experimental study looking at porosities within carbon fiber reinforced polymer laminates [7] and was specifically looking at porosities ranging from 0.8-3.4%. In their study, all mechanical properties were lowered as porosity increased by between 0.9-20.8%, but shear was affected far more than tensile stresses. A fourth paper [8] on porosity within vacuum-bag fiber-reinforced polymer panels showed that between the porosities of 1.5% to 3.4% fracture toughness decreased by 13% and fatigue life dropped by 50%.

1.3 Tested Systems and Parameters of Interest

The purpose of this study was to compare the porosity found within samples produced on five different single-screw extruder systems. These systems were the Big Area Additive Manufacturing (BAAM) system at the MDF, an IM machine and a separate vented screw test extruder both belonging to Techmer PM, a proprietary commercial system, and finally a few archived samples from an older selectively vented extruder. All samples analyzed for this study were ABS 20 % carbon fiber with the exception of the archived samples whose precise composition was not available. Various extrusion parameters were controlled within each system allowing for a comparison of their effects on porosity. These parameters were drying methods, pressure, venting, and extrusion rates including the effects of changing extrusion rates in the form of transient vs steady state flow. The primary focus of the study was on the samples from the BAAM system. The other four extruders were each examined for the purpose of comparison or to study the affects of factors BAAM does not currently have the capability to adjust.

1.4 Sample Descriptions by System

1.4.1 BAAM

The BAAM is a large-scale single screw extruder produced by Cincinnati and housed at the MDF of ORNL. The seven single bead samples produced for this study were approximately 1m (3ft) long and printed at varying screw speeds ranging from 50 rpm – 350 rpm in 50 rpm increments. These were then sectioned in three locations the first inch of the bead, the middle middle, and the inch at the end of each bead just prior to a large deformation resulting from the extruder head halting and depositing extra material as it lifted off the platform. This resulted in 21 sets of two samples: both surfaces exposed by sectioning made up each set. The three locations were chosen to examine the effects of transient flow at three times within the print run: as the polymer first began to flow, once the polymer reached steady state, and as the system slowed down at the end of the bead. The pellet feedstock for these prints was dried at approximately 65ºC (150ºF) for 12hr in a desiccant dryer.

1.4.2 Techmer PM

Two systems at the Clinton Plant of Techmer were used. The first was a single screw injection molding machine, and the other was a similarly proportioned single screw extruder outfitted with a vent in the side of the barrel. One standard tensile bar was produced via injection molding with a final molding pressure of 13.5k psi. The screw feedrate was 13.7 m/min (9 in/sec). The sample was sectioned from the center of the tensile bar. Just prior to molding the bar, an "airshot" was performed where the polymer was ejected directly into atmospheric pressure from the extruder for a few seconds. A sample of the 3mm bead produced was collected. A sample from a second airshot performed on a vented test extruder was also collected. The vent was 0.41m (16in) from the output nozzle of the extruder and was open to atmospheric pressure (as opposed to an induced vacuum). Four beads from each airshot were mounted and analyzed. The pellet feedstock for these samples had been dried at 70ºC (158ºF) for 2hr without the use of desiccants.

1.4.3 Commercial System

The samples from this commercial single screw extrusion system were provided for this study under the conditions that the specifics of the system remain unpublished for now. The three provides samples were multi-bead walls extruded from a 4mm nozzle at feedrates of 2k, 6k, and 10k mm/min (1.31, 3.94, and 6.56 in/sec respectively) were provided. Three beads at each feedrate were sectioned and analyzed. Similarly to the BAAM samples, both surfaces exposed during sectioning were mounted providing a total of 6 samples per feedrate.

1.4.4 Archived Samples

Two images from an older extruder were analyzed. The system that produced them had been capable of switching between vented and non-vented extrusion. The original print parameters of the samples were largely unavailable. What was known was that the samples were identical except one sample was vented, and the other was not.

2. EXPERIMENTATION

2.1 Sample Preparation

Each physical sample from each system differed significantly in size and shape. The BAAM samples were single flattened beads measuring about 1.5cm wide by 2-3mm thick (Figure 4). The Techmer airshots from the two extruders were 3mm diameter cylindrical beads and the injection molded bar was a 4mm by 10mm rectangle. The commercial system provided multi bead wide but single bead tall walls. Each sample regardless of dimensions was sectioned to approximately 1cm in length on an Allied TechCut 5TM Precision High Speed Saw using a diamond wafering blade at 1000rpm for the blade and a feedrate of between 0.021 mm/s (0.05 in/min) and 0.064 m/sec (0.15 in/min). A slower feedrate protects the internal fibers from shattering. If fibers are too badly damaged this can result in higher fiber pullout as fragments of broken fibers fall out of the polymer matrix during the polishing procedure. These

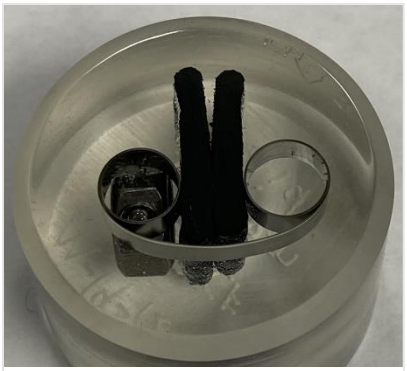

Figure 4, Two adjacent BAAM Samples mounted in a 32 mm epoxy puck

fragments can result in polishing defects because they can be drug across the surface during the polishing resulting in scratches of varying severity. Fiber pullout is also a cause of false positives during porosity measurement as the fibers leave behind small holes in the matrix. To determine if fiber pullout was a concern, a typical multi-bead wall of fiber reinforced ABS from the BAAM was sectioned in two distinct ways. One sample was sectioned at 0.021 mm/s on the TechCut, and the other was the was sectioned with a bandsaw. Both samples were mounted in epoxy, and the sample surface of each was ground and polished. The grinding worked from 250grit for 2min all the way to 4000k grit for 15min and removed approximately 3.2 mm (1/8th in) of material. They were polished with a 5µm diamond slurry for 25min. After both samples were imaged and analyzed (process explained next), their average porosity across multiple sections of each sample, each contained three printed beads, was found to be 17.5 % and 17.7 % differing by only 0.2 %. It should be noted that no significant scratching occurred from fiber fragments, so the only concern was the effect of false positives from fiber pullout. This indicated that the grinding and polishing procedure removed enough material to minimize the negative effects of rough or rapid sectioning on the surface of the sample. An example of a pair of mounted and polished BAAM samples can be seen in Figure 4.

2.2 Porosity Measurement through Optical Micrographs and Image Analysis

Two optical microscopes were used to image the samples for this study; a Zeiss Axio Imager and a Leica DM4000M. At total magnifications between 200x-300x, the Axio provided clearer images with higher feature contrast that were easier to analyze compared to those provided by the Leica, but both were acceptable. The key controls used for the analysis were exposure time, lighting intensity, gamma correction, and multi-focus stitching. There was no universal set of settings that would work for all samples. The goal during the image capturing process was to achieve as high a pixel-value contrast between porosity and all other features as possible such that a pixel value threshold could be detected that would isolate porosity within the image. Exposure time and lighting were set by starting them at the default setting and then adjusting them to have longer duration and higher intensities until the background polymer matrix was as close to the same pixel value as the fibers within the matrix. One concern during this adjustment was ensuring that the porosity was not being washed out. This would occur depending on the average depth or size of the pores within the specific sample; shallow pores were easy to wash out and lose, so for some samples the optimal contrast between porosity and background could not be achieved. Gamma correction refers to a post-processing feature built into both microscopes used for this study. It allows the user to skew the distribution of pixel values captured by the microscope. A gamma value between 0 and 1 skews the resulting image to have far more pixel values assigned to the dark regions of the image (low pixel values), while a gamma above 1 results in an image where more of the pixel value range is assigned to the bright regions of the image. For the purposes of this study, the feature of interest was porosity which appears as shadows or regions of very low brightness/pixel values. Therefore, a gamma value of between 0.2 and 0.3 was used to further increase the contrast difference between porosity and all other features. Figure 5 shows an image captured on the Axio imager that clearly displays the desired high contrast between the dark regions of porosity and the bright background matrix and fibers (small white dots).

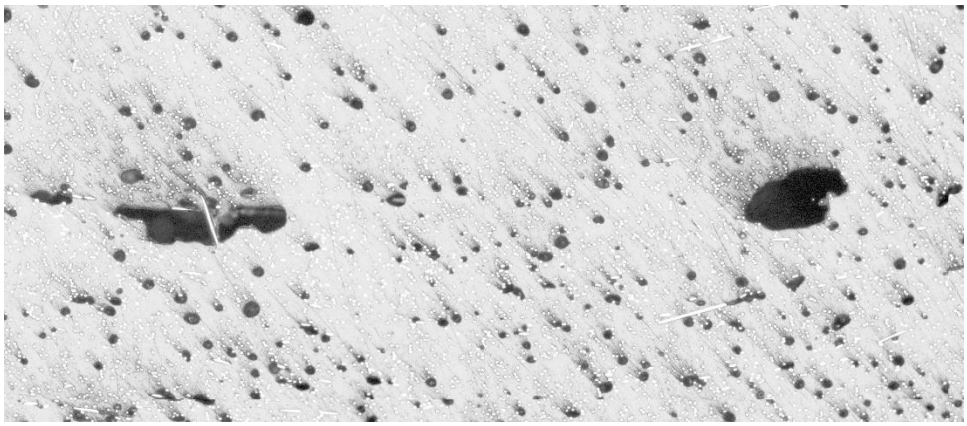

Figure 5. A small section of an image captured on the Axio Imager

The Fiji distribution of ImageJ [9] was used to perform the image analysis. The base distribution would have been sufficient for the analysis that was completed. The following generalized process was used and adjusted for each set of sample images.

1. Start by cropping a rectangular region of interest out of your total image that avoids polishing defects or other unwanted features.
    a. Rectangular sections do result in missing porosities near heavily curved surfaces but can be analyzed far more efficiently by converting these steps into a repeatable macro with Fiji's built in macro creator.
2. Set the image to be an 8-bit black and white image.
    a. Several of the following tools can only function on an 8-bit image
3. Create a copy of the new 8-bit image.
4. Subtract a value of 1 from all pixels in the copy. This will result in all pixels with the value of 0 and 1 having the value of 0 and no pixels having the maximum value of 255.
5. Return to the original 8-bit image and run the process "subtract background" with a radius of 5 pixels.
    a. This is intended to help smooth out any uneven lighting in the background of the image that may negatively effect the thresholding of the image.
6. Apply an automatic threshold.
    a. There are multiple options available and depending on the precise lighting and contrast you managed to achieve through microscopy, different ones will prove to be more effective.
    b. In this study images captured on the Axio used the default threshold while those taken with the Leica needed to use the "MaxEntropy" setting to accurately identify the porosity.
7. This produces a binary image with all porosity being assigned a pixel value of 255 and the rest of the image being assigned a value of 0.
8. Run the "Analyze Particles" tool. Chose the options for "show masks" and "include holes."
    a. Optional: set a minimum particle pixel size to eliminate "salt and pepper" defects resulting from the edges of fibers or other minor surface defects that were included in the threshold. This trades the error of overestimating porosity due to false positives for the error of not including porosities smaller than the cutoff.

b. For this study, for each set of images (with shared microscope settings), a minimum particle size was set by measuring size of several manually selected defects. This typically ranged from 100-150pixels.
c. The option to “include holes” fills in pores that only appear as outlines after thresholding. This often would occur when the pores were very shallow or wide and the bottom of the pore would reflect back more light to the sensor, appear brighter than desired, and be missed by the threshold.

9. Add the “mask” created in step 8 to the edited copy created in step 4. To determine the porosity as a percentage of surface area, divide the number of pixels with a value of 255 from the total pixel count of the image.
    a. Now you have a single image where all detected porosity has been assigned a pixel value of 255, and the remainder of the image remains intact (but reduced in pixel value by 1 compared to the original).

Figures 6 and 7 show the before and after of these 9 steps.

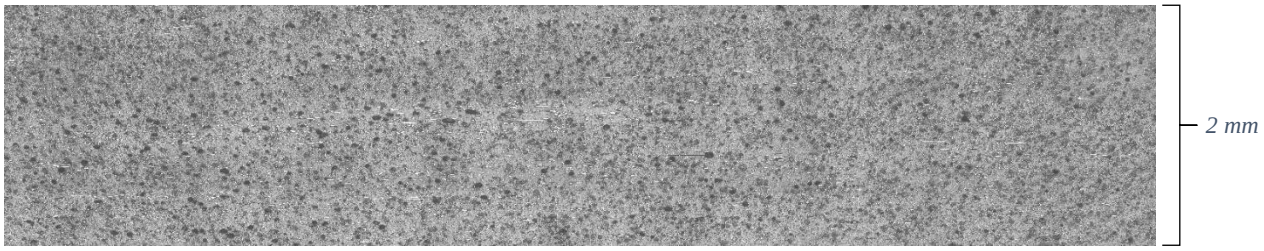

Figure 6. A rectangular section of a BAAM sample to be analyzed

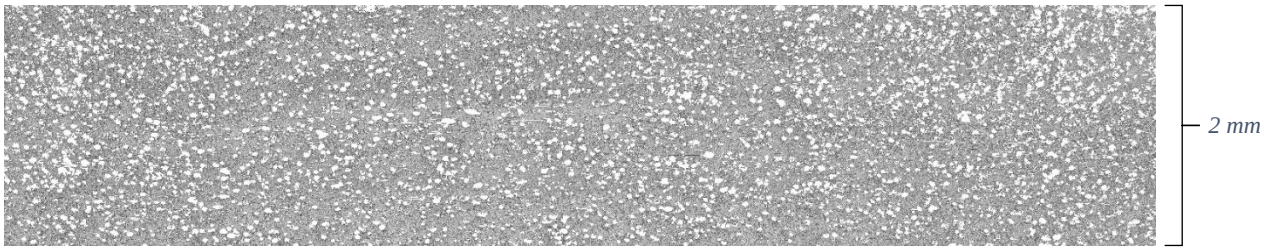

Figure 7. Porosity isolated as the only pixels at a value of 255

3. RESULTS

3.1 BAAM

Figure 8 summarizes the collected data from the porosity analysis. The primary variables being examined were screw speeds (and therefor flowrates) and transient vs steady state effects. Seven screw speeds were tested and samples were taken from the first inch of the extruded material, the middle of the extruded bead, and just prior to a large material deformation formed as the extruder nozzle came to a halt at the end of each bead. The effects of transient flow can be clearly seen as the porosity at the start of each bead was consistently higher than further along the bead. A second pattern is that the porosity becomes significantly more erratic as the screw speed passes 200 rpm. As the screw speed ramps from 50 rpm to 200 the porosity decreases. It also decreases at the end of the bead relative to the start of the bead for this rpm range. After 200 rpm, the porosities increase again, but with a higher variance than before. The data at the end of each bead was inconclusive

as to whether transient effects occur as the system comes to a halt. This could be because the samples were taken from just prior to the large geometric deformation of the bead caused by the print head halting, lifting, and dragging material along with it. Any potential end effects could be caught up in that deformation but taking samples from within the deformation would result in measurements with far more unknowns. Overall, porosities ranged from 4.3 % (middle of the bead at 250 rpm) to 7.5 % (start of the bead at 50 rpm).

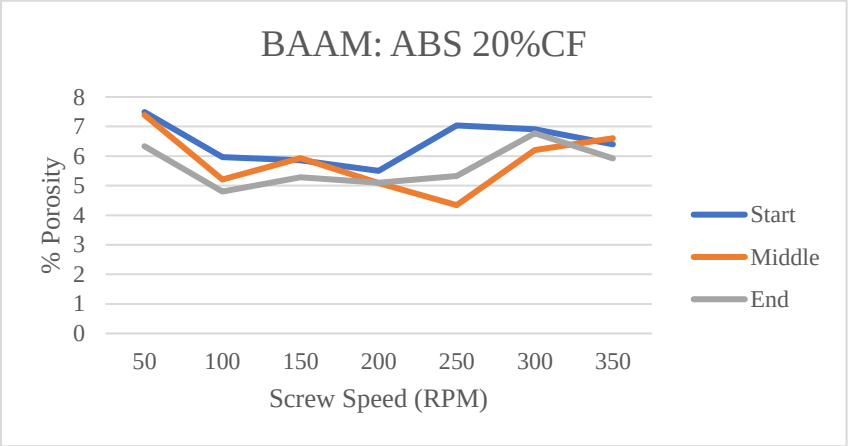

Figure 8. Porosity as a function of Screw Speed and Sample Location along the extruded bead

3.2 Techmer

The Techmer samples were produced on injection molding equipment allowing a direct comparison to the industry from which pellet fed AM is derived. The low porosity molded bars show how gasses can be kept dissolved within the polymer by maintaining pressure, and the high porosity airshots show how much gas was contained within that polymer. All three samples were extruded from the same batch of pellet feedstock on the same day no more than 20min apart. This is important to note considering the variance in porosities produced across these samples. The molded bar (Figure 9) had only 0.1 % porosity, while the airshot produced from the same machine seconds prior averaged 16.7 %. The vented airshot averaged 0.3 % which is still higher than the molded bar but is 98% lower than the non-vented airshot. Figures 10 shows the high porosity within a non-vented airshot while Figure 11 shows a relatively pore free vented airshot. Table 1 summarizes the measured porosities. It should be noted that the porosity of the Techmer airshot was close to 17 % while the BAAM samples produced with the same material maxed out at about 7.5 %. A few possible explanations include moisture content, nozzle size, or extrusion feedrate. Of these, the most likely variable is moisture content because the BAAM samples were dried for 6 times the duration at a similar temperature with the aid of desiccants.

Table 1, Collected data from Techmer samples

	Average %	Min %	Max %
Molded	0.1	n/a	n/a
Non-Vented	16.7	15.5	17.8
Vented	0.3	0.1	0.4

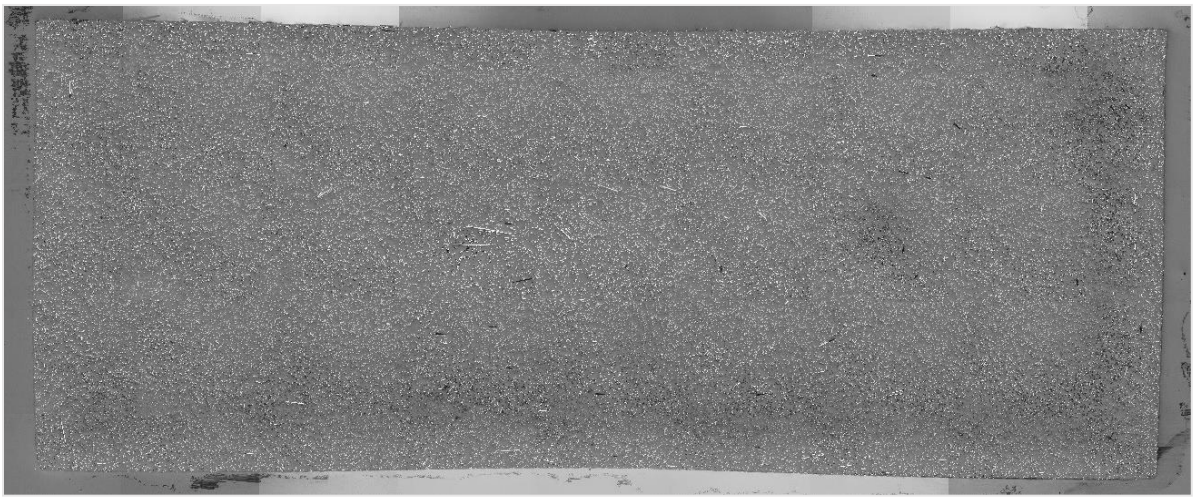

Figure 9, Techmer Molded Bar

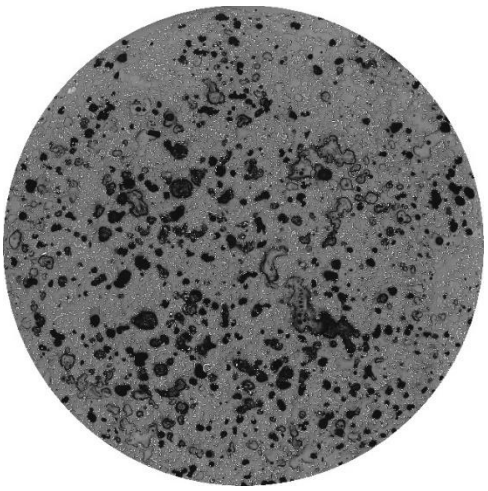

Figure 10, Non-Vented Techmer Airshot

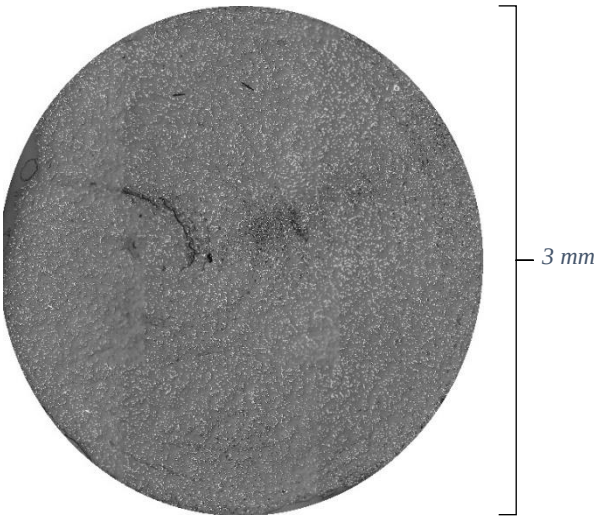

Figure 11, Vented Techmer Airshot

3.3 Commercial System

The primary purpose of the samples from the commercial system was as a second look at the effects of flow rates on porosity to compare to BAAM. Figure 12 shows a box and whisker plot of the porosity at each tested feedrate. As the feedrate increased, so did the porosity. At the highest feedrate of 10k mm/min there was also an increase in the variance of the porosity from 1.7% at 2k mm/min and 1.9% at 6k mm/min to 4.5%. Figures 13-15 show how the porosity can be seen to increase as feed rate also increased. The bead depicted was chosen for being closest to the average porosity for that rate. Table 2 shows the average, minimum, and maximum porosities at each feedrate. The control scheme of BAAM is based on screw speeds while the commercial system controlled the feedrate of the material. Going forwards, further studies could include additional measurements to allow for a measurement of volumetric flowrate which would allow for a more direct comparison between systems. This would be particularly useful when trying to understand why the commercial system showed exclusively an increase in porosity as feedrate was increased, but BAAM showed two regions of differing behavior at low vs high feedrates.

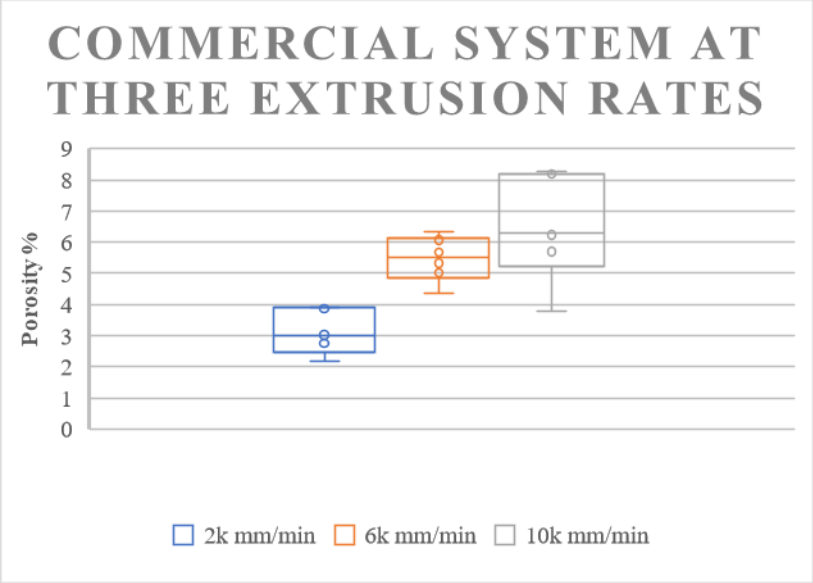

Figure 12, Porosity % and Variance of a Commercial System

Figure 13, Single bead at 2k mm/min

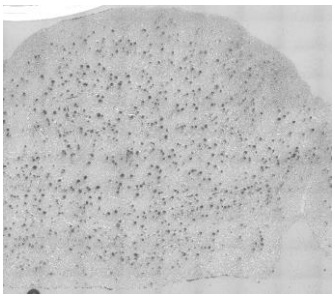

Figure 14, Single Bead at 6k mm/min

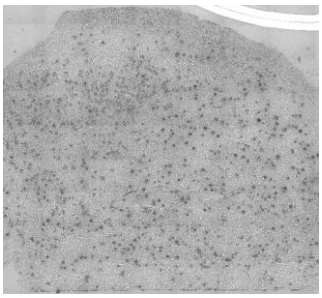

Figure 15, Single bead at 10k mm/min

Table 2, Summarized Porosity data from Commercial System

	Average %	Min %	Max %
2k mm/min (1.31 in/sec)	3.2	2.2	3.9
6k mm/min (3.94 in/sec)	5.5	4.4	6.3
10k mm/min (6.56 in/sec)	6.4	3.8	8.3

3.4 Archived Sample Images

The archived images from this system are valuable because they provide an example of the effectiveness of venting on porosity. Table 3 lists the porosities for the two archived samples depicted in Figures 16 and 17. Using a vented system the overall porosity dropped from 18.4% to 6.6%, a 64% total reduction. These archived samples show that even after venting, porosity is not always eliminated as efficiently as it was in the Techmer samples. The reason for this discrepancy could not be determined due to the limited data on the archived samples.

Table 3, Porosity for each Archived Sample

	Porosity %
Non-Vented	18.4
Vented	6.6

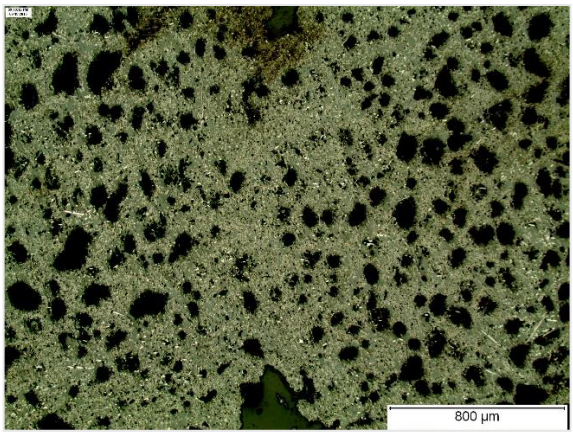

Figure 16, Archived Non vented sample: 18.4% Porosity

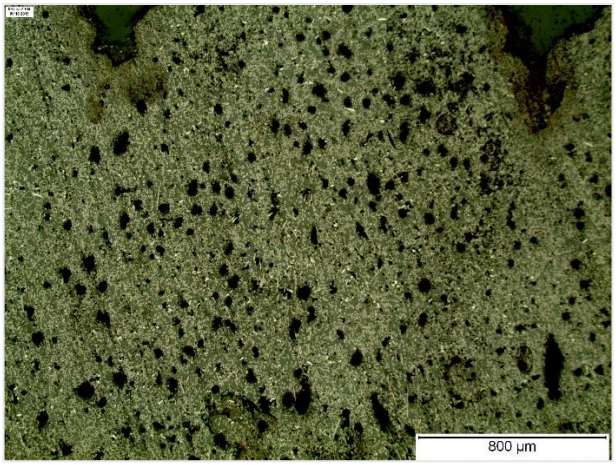

Figure 17, Archived Vented Sample: 6.6% Porosity

4. CONCLUSIONS

4.1 Feedrates

There are clear trends between feedrates and porosity in both the commercial system and BAAM samples. In both cases, there was an increase in the average porosity and the variance of porosity within each set of samples at high feed rates, but BAAM suggests that this might not hold true at low feedrates.

4.2 Transients

The positional data from the BAAM samples showed that transient flow results in higher porosity. Further research needs to be done to determine the duration of these effects.

4.3 Gasses and Moisture

Comparing the non-vented airshot from Techmer to the injection molded bar indicates that most of the porosity can be attributed to the pressure the samples were allowed to solidify at. At the high pressures of the mold, any dissolved gasses or moisture appear to have remained in solution even after the solidified part was removed from the pressure chamber, while they expanded to form porosity as soon as they were exposed to atmospheric pressures during the airshot.

4.4 Venting

Of all the parameters tested, venting showed the most promise for reducing porosity with total reductions of 64% in the archived samples and 98% for the vented Techmer airshots.

5. REFERENCES

1. Rauwendaal, Chris. “Polymer Extrusion”. Carl Hanser Fachbuchverlag, 2014.
2. Clémence Nikitine, Elisabeth Rodier, Martial Sauceau, Jean-Jacques Letourneau, Jacques Fages, “Controlling the structure of a porous polymer by coupling supercritical CO2 and single screw extrusion process” in *Journal of Applied Polymer Science*, Sep. 15, 2009, https://doi.org/10.1002/app.31031
3. DeNardo, Nicholas M., "Additive manufacturing of carbon fiber-reinforced thermoplastic composites" (2016). Open Access Theses. 939. https://docs.lib.purdue.edu/open_access_theses/939
4. Greger Nilsson, S. Patrik Fernberg, Lars A. Berglund, “Strain field inhomogeneities and stiffness changes in GMT containing voids”, doi.org/10.1016/S1359-835X(01)00056-2
5. K. A. Chowdhury, R. Talreja, A. A. Benzerga, “Effects of Manufacturing-Induced Voids on Local Failure in Polymer-Based Composites”, DOI: 10.1115/1.2841529
6. Gaétan Dalongeville, Mouhamadou Dabo, Christian Gauthier , Thierry Roland, “Propriétés mécaniques des mousses polymères : influence de l'architecture interne sur les raideurs.”, https://cfm2017.sciencesconf.org/133493.html
7. AG Stamopoulos, KI Tserpes, P Prucham, D Vavrik, “Evaluation of porosity effects on the mechanical properties of carbon fiber-reinforced plastic unidirectional laminates by X-ray computed tomography and mechanical testing”, journals.sagepub.com/doi/pdf/10.1177/0021998315602049
8. Hakim, I.A., Donaldson, S.L., Meyendorf, N.G. and Browning, C.E. (2017) “Porosity Effects on Interlaminar Fracture Behavior in Carbon Fiber-Reinforced Polymer Composites.” Materials Sciences and Applications , 8, 170-187. https://doi.org/10.4236/msa.2017.82011
9. Schindelin, J.; Arganda-Carreras, I. & Frise, E. et al. (2012), "Fiji: an open-source platform for biological-image analysis", *Nature methods* **9(7)**: 676-682, PMID 22743772, doi:10.1038/nmeth.2019 (on Google Scholar).

Acknowledgments:

1) This research was supported in part by an appointment to the *HERE Program* at Oak Ridge National Laboratory. (Statement required as part of internship)

2) Research sponsored by the U.S. Department of Energy, Office of Energy Efficiency and Renewable Energy, Advanced Manufacturing Office, under contract DE-AC05-00OR22725 with UT-Battelle, LLC.